

Towards a better knowledge of the nuclear equation of state from the isoscalar breathing mode

E. Khan¹ and J. Margueron^{1,2}

¹*Institut de Physique Nucléaire, Université Paris-Sud, IN2P3-CNRS, F-91406 Orsay Cedex, France*

²*Institut de Physique Nucléaire de Lyon, Université de Lyon, IN2P3-CNRS, F-69622 Villeurbanne, France*

(Dated: July 16, 2018)

The measurements of the isoscalar giant monopole resonance (GMR), also called the breathing mode, are analyzed with respect to their constraints on the quantity M_c , e.g. the density dependence of the nuclear incompressibility around the so-called crossing density $\rho_c=0.1 \text{ fm}^{-3}$. The correlation between the centroid of the GMR, E_{GMR} , and M_c is shown to be more accurate than the one between E_{GMR} and the incompressibility modulus at saturation density, K_∞ , giving rise to an improved determination on the nuclear equation of state. The relationship between M_c and K_∞ is given as a function of the skewness parameter Q_∞ associated to the density dependence of the equation of state. The large variation of Q_∞ among different energy density functionals directly impacts the knowledge of K_∞ : a better knowledge of Q_∞ is required to deduce more accurately K_∞ . Using the Local Density Approximation, a simple and accurate expression relating E_{GMR} and the quantity M_c is derived and successfully compared to the fully microscopic predictions.

PACS numbers: 21.10.Re, 21.65.-f, 21.60.Jz

I. INTRODUCTION

The determination of the nuclear incompressibility is a long standing problem. The earliest microscopic analysis came to a value of $K_\infty=210 \text{ MeV}$ [1], but with the advent of microscopic relativistic approaches, a value of $K_\infty=260 \text{ MeV}$ was obtained [2]. The fact that K_∞ cannot be better determined than $230\pm 40 \text{ MeV}$, taking into account the whole data on the isoscalar Giant Monopole Resonance (GMR) as well as the various methods to relate the GMR to K_∞ (see e.g. [1–9]) lead to a recent effort to reanalyse the method [10].

Pairing effects and similarly the shell structure effects on the nuclear incompressibility were analyzed along these lines. Since the first investigation [11], several studies have shown that pairing effects have an impact on the determination of K_∞ [7, 8], and it was considered as a possible cause of the difficulty to accurately constrain K_∞ . This effect of pairing on the incompressibility modulus has also been analyzed in nuclear matter, showing that the main effect is occurring at subsaturation densities [12]. However there is a general consensus between the various microscopic models that pairing effects on K_∞ are not strong enough to explain the lack of accuracy in the determination of the nuclear incompressibility [7–9, 13]. Other effects have to be investigated.

Recently, the density dependence of the nuclear incompressibility was re-investigated suggesting that the correlation between the centroid of the GMR and the incompressibility modulus K_∞ at saturation density is blurred by the density dependence of the nuclear equation of state in different models [10]. The observed differences in the extraction of K_∞ from the E_{GMR} are based on different models and attributed to the density dependence of the equation of state (EoS) which has still to be better constrained. The observation of a crossing point provided a possible path to be investigated. The crossing point

arises from Energy Density Functionals (EDFs) that are designed to describe finite-nuclei observables: their density-dependent incompressibility $K(\rho)$ crosses around the mean density in nuclei, $\rho_c \simeq 0.1 \text{ fm}^{-3}$. It was therefore proposed that the quantity M_c , e.g. the density dependence of $K(\rho)$ around the crossing density ρ_c is the quantity that shall be constrained by measurements of the GMR, instead of K_∞ .

The aim of the present article is to further analyze the correlation method on which is extracted the incompressibility modulus K_∞ , and to give a better basis on the alternative method based on the correlation between E_{GMR} and M_c . A comparison between the two methods is given in Sec. II for ^{208}Pb and ^{120}Sn nuclei, showing the relevance of the new method [10]. In Sec. III the source of uncertainties in the determination of K_∞ is directly related to the skewness parameter Q_∞ . The skewness parameter gives indeed the present limitation on the knowledge of the density dependence of the nuclear EoS between the crossing and the saturation densities. The origin of the crossing density is also demonstrated in the case of the Skyrme EDFs. In Sec. IV, the explicit relation between the centroid of the GMR and the quantity M_c is derived using the Local Density approximation (LDA), and keeping as much as possible analytical relations between the various quantities, in order to facilitate their interpretation. The results are compared to the fully microscopic one. Conclusions are given in Sec. V.

II. THE MICROSCOPIC APPROACH

In this section, we first summarize the Constrained Hartree-Fock-Bogoliubov approach (CHFb) used to accurately predict the Isoscalar Giant Monopole Resonance (GMR) energy. We then provide the definition of the parameter M_c , driving the density dependence of the in-

compressibility around the crossing point. Finally, using these two quantities, the correlation analysis between the GMR energy and the incompressibility modulus K_∞ on one hand, and the GMR energy and the parameter M_c at the crossing density on the other hand, are compared.

A. Microscopic calculation of the GMR energy

We first recall how to predict the E_{GMR} . We use the sum rule approach in order to microscopically calculate the centroid energy of the GMR. In such a microscopic approach, we calculate the energy as

$$E_{\text{GMR}} = \sqrt{\frac{m_1}{m_{-1}}}. \quad (1)$$

where the k -th energy weighted sum rule is defined as

$$m_k = \sum_i (E_i)^k |\langle i | \hat{Q} | 0 \rangle|^2, \quad (2)$$

with the RPA excitation energy E_i and the isoscalar monopole transition operator,

$$\hat{Q} = \sum_{i=1}^A r_i^2. \quad (3)$$

The calculations using fully microscopic approaches based on EDF are usually performed using CHFB or the RPA approach [14]. In the present case we calculate the GMR centroid for the Skyrme EDF with the CHFB approach. For completeness, results using other functionals such as Gogny and relativistic functionals will also be given. The CHFB method is known to provide an accurate prediction of the GMR centroid.

In the following the energy weighted moment m_1 and the m_{-1} moment are directly evaluated from the ground-state obtained from Skyrme CHFB calculations. The moment m_1 is evaluated by the double commutator using the Thouless theorem [15]:

$$m_1 = \frac{2\hbar^2 A}{m} \langle r^2 \rangle. \quad (4)$$

where A is the number of nucleons, m the nucleon mass and $\langle r^2 \rangle$ is the rms radius evaluated on the ground-state density given by Skyrme HFB.

Concerning the evaluation of the moment m_{-1} , the constrained-HFB approach is used. It should be noted that the extension of the constrained HF method [4, 16] to the CHFB case has been demonstrated in Ref. [17] and employed in [8]. The CHFB Hamiltonian is built by adding the constraint associated with the isoscalar monopole operator, namely

$$\hat{H}_{\text{constr.}} = \hat{H} + \lambda \hat{Q}, \quad (5)$$

and the m_{-1} moment is obtained from the derivative of the expectation value of the monopole operator on the

CHFB solution $|\lambda\rangle$,

$$m_{-1} = -\frac{1}{2} \left[\frac{\partial}{\partial \lambda} \langle \lambda | \hat{Q} | \lambda \rangle \right]_{\lambda=0}. \quad (6)$$

B. Constraints on the equation of state deduced from E_{GMR}

Next, the parameter M_c is defined. Instead of correlating E_{GMR} and K_∞ , it was proposed that the energy of the GMR (1) gives a strong constraint on the quantity M_c defined, at the crossing density $\rho_c \simeq 0.1 \text{ fm}^{-3}$, as [10],

$$M_c \equiv 3\rho_c K'(\rho)|_{\rho=\rho_c}, \quad (7)$$

where the density-dependent incompressibility $K(\rho)$ is derived from the thermodynamical compressibility $\chi(\rho)$ as [18],

$$K(\rho) = \frac{9\rho}{\chi(\rho)} = \frac{18}{\rho} P(\rho) + 9\rho^2 \frac{\partial^2 E(\rho)/A}{\partial \rho^2}, \quad (8)$$

and the pressure is

$$P(\rho) \equiv \rho^2 \frac{\partial E(\rho)/A}{\partial \rho} \quad (9)$$

The parameter M_c was introduced instead of $K_\infty \equiv K(\rho_0)$ (where ρ_0 is the saturation density) in the correlation analysis based on E_{GMR} since i) the crossing density ρ_c is closer to the average density in finite nuclei than the saturation density ρ_0 , and ii) the crossing of the incompressibility at ρ_c makes the E_{GMR} mostly sensitive to the derivative of the incompressibility at the crossing density [10]. It should be noted that the existence of a crossing density for other EoS quantities, such as for instance the symmetry energy [19], the neutron EoS [20, 21] and the pairing gap in nuclear matter [22], was also observed. It might reveal the general trend that the experimental constraints drive these quantities towards a crossing point at around the average density of finite nuclei. Various EDF's shall however exhibit various density dependencies around the crossing point. At first order the derivative of the incompressibility (or symmetry energy or pairing gap) at this point will differ between various EDF's and additional measurements in nuclei shall characterize these derivatives. For instance, the derivative of the neutron EoS around $\rho_c \simeq 0.11 \text{ fm}^{-3}$ was found to be strongly correlated to the neutron skin in ^{208}Pb [20, 21], giving a strong support to improved experimental measurements of this quantity [23].

Fig. 1 depicts $K(\rho)$, between half of the saturation density and the saturation density, for several Gogny, Skyrme and relativistic EDFs. A large dispersion is observed at saturation density ($\rho/\rho_0 = 1$) whereas at $\rho/\rho_0 \simeq 0.71$ there is a much more focused area, defining the crossing density ρ_c .

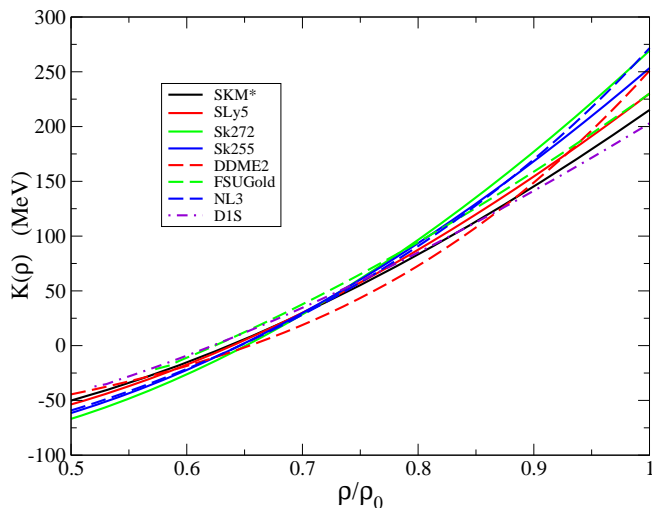


FIG. 1. (Color online) EoS incompressibility $K(\rho)$ calculated with various relativistic and non-relativistic functionals. The Skyrme EDF are in solid lines

We now analyze the two contributions to the density-dependent incompressibility, as depicted by Eq. (8). The first term of the r.h.s in Eq. (8) is proportional to the pressure $P(\rho)$, which is indeed related to the first derivative of E/A and the second term is the second derivative of the binding energy E/A with respect to the density. The former vanishes at saturation density, by definition. Table I displays the expectation values of these two contributions to the incompressibility $K(\rho)$ (Eq. (8)) at the crossing density $\rho_c = 0.71\rho_0$ and at the saturation density for several EDFs. The total value of $K(\rho_c) \equiv K_c$ at the crossing density is also displayed, while at ρ_0 , $K_\infty = 9\rho_0^2 \frac{\partial^2 E(\rho)/A}{\partial \rho^2} |_{\rho_0}$. The very weak dispersion of K_c as a function of the EDFs is striking, whereas the incompressibility modulus at the saturation density K_∞ is more scattered. At the crossing density, the incompressibility K_c is given as the sum of the first and second derivatives of the energy per particle E/A , which act in opposite signs, see Table I. The contribution of the pressure at ρ_c is not negligible, at variance with its contribution at ρ_0 , and largely contributes to the stabilisation of K_c . The correlations between E_{GMR} and the solely second derivative of E/A at the saturation density might not be the most appropriate one and the EDF-invariant property of the crossing point (ρ_c, K_c) shall be useful.

C. $(E_{\text{GMR}}, K_\infty)$ versus (E_{GMR}, M_c) correlation analysis

Using E_{GMR} and M_c discussed in the previous sections, it is possible to determine if M_c is better constrained by E_{GMR} than K_∞ . The correlation diagrams $(E_{\text{GMR}}, K_\infty)$ and (E_{GMR}, M_c) are compared on Fig. 2 in the case of ^{208}Pb . The relativistic DDME2 interaction in the cor-

	Crossing			Saturation		
	K_c	$\frac{18}{\rho_c} P(\rho_c)$	$9\rho_c^2 \frac{\partial^2 E(\rho)/A}{\partial \rho^2} _{\rho_c}$	K_∞	$P(\rho_0)$	$9\rho_0^2 \frac{\partial^2 E(\rho)/A}{\partial \rho^2} _{\rho_0}$
	MeV	MeV	MeV	MeV	MeV	MeV
SLy5	36	-103	139	230	0	230
SkM*	34	-99	133	217	0	217
Sk255	36	-113	149	255	0	255
Sk272	35	-119	154	272	0	272
SGII	34	-98	132	215	0	215

TABLE I. Evaluation of K_c and of the two terms defining the incompressibility $K(\rho)$ (Eq. (8)), at the crossing density $\rho_c = 0.71\rho_0$ and at the saturation density ρ_0 for a set of different Skyrme EDFs.

relation graph $(E_{\text{GMR}}, K_\infty)$ is largely deviating from the others, as it is well known [2–4] while it is much more compatible with the others in the (E_{GMR}, M_c) correlation graph [10]. On the contrary, restricting to the Skyrme interactions, the quantities $(E_{\text{GMR}}, K_\infty)$ and (E_{GMR}, M_c) are equally well correlated. This is directly related to the good correlation between (M_c, K_∞) due to a similar density dependence among the Skyrme EDFs (in ρ^α), which will be discussed in section III.C. However, considering various models with different density dependencies, a better correlation is observed between E_{GMR} and M_c , compared to the one between E_{GMR} and K_∞ . It should be noted that in the (E_{GMR}, M_c) correlation graph, an ordering between Skyrme and relativistic models is also observed.

Fig. 3 displays the same correlations in the case of the ^{120}Sn nucleus. In this case pairing effects are known to slightly impact the position of the GMR [12], leading to a larger dispersion compared to the ^{208}Pb case. However similar conclusions can be drawn, namely i) M_c is a better correlated quantity with E_{GMR} than K_∞ , ii) a good $(E_{\text{GMR}}, K_\infty)$ correlation is also observed among the Skyrme interactions and iii) the (E_{GMR}, M_c) correlation exhibits an ordered correlation between the Skyrme and the relativistic EDFs.

To conclude, these results on M_c provide a step towards compatible results between Skyrme, Gogny and relativistic approaches [10]. The extracted value for the quantity M_c in ^{120}Sn and ^{208}Pb nuclei are also in better agreement between each other than the corresponding K_∞ values: considering the various EDFs as well as the ^{120}Sn and the ^{208}Pb data, one gets $M_c = 1100 \pm 70$ MeV (6% uncertainty), and $K_\infty = 230 \pm 40$ MeV (17% uncertainty) [10]. It should be noted that these considerations on the slope of the incompressibility M_c at the crossing point have recently been used in Ref. [29] where a good linear correlation between E_{GMR} and M_c is also found, including the so-called BCPM functional.

In summary, using microscopic approaches, it is observed that the correlation between M_c and the centroid

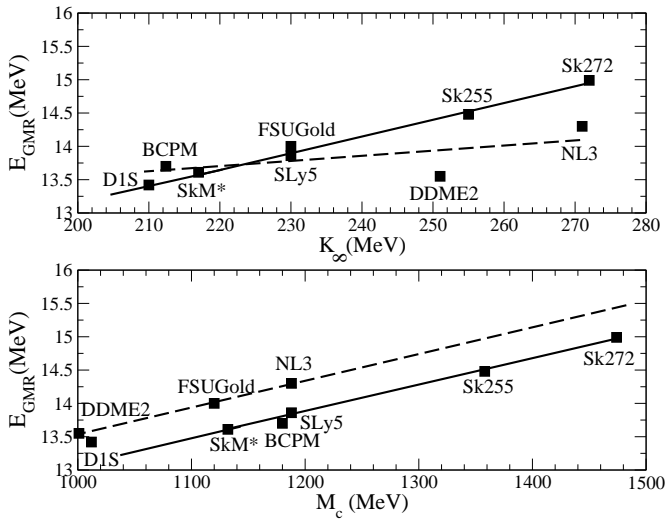


FIG. 2. Centroid of the GMR in ^{208}Pb calculated with the microscopic method (see text) vs. the value of K_∞ (top) and M_c (bottom) for various functionals [3, 5, 10, 24–29]. The solid and dashed lines correspond to fit on the Skyrme and relativistic EDF values, respectively.

E_{GMR} is less dispersive, and therefore more universal among various models, than the one between K_∞ and E_{GMR} [10]. In the next section, we shall provide a more quantitative understanding of the differences between the quantities M_c and K_∞ , explaining the role of the density dependence of the equation of state between the crossing and the saturation densities.

III. DENSITY EXPANSION OF THE EQUATION OF STATE

The striking stability of K_c among the various Skyrme EDFs (Table I) deserves an investigation. In this section, the density dependence of the equation of state is discussed in terms of the derivatives of the EoS with respect to the density. The stability of K_c as well as the relation between the slope of the incompressibility modulus M_c and the parameters K_∞ and Q_∞ are derived, providing an explanation for the difficulty to constrain K_∞ .

A. Density dependence of the equation of state around ρ_0

We start from a systematic expansion around the saturation density ρ_0 of the binding energy, such as in the Generalized Liquid Drop Model (GLDM) [30, 31] where, in symmetric matter, the energy per particle reads

$$E(x) = E_\infty + \frac{1}{2}K_\infty x^2 + \frac{1}{6}Q_\infty x^3 \dots \quad (10)$$

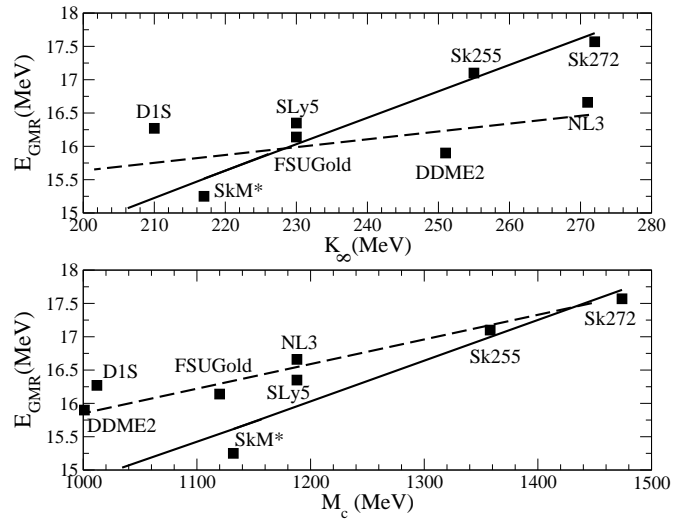


FIG. 3. Same as Fig. 2 for ^{120}Sn .

with $x = (\rho - \rho_0)/(3\rho_0)$, ρ_0 being the saturation density of symmetric nuclear matter. Q_∞ is the third derivative of the energy per particle.

Applying Eqs. (8) and (9) to the expansion Eq. (10), one obtains the pressure,

$$P(x) = \frac{1}{3}(1 + 3x)^2 \left[K_\infty x + \frac{1}{2}Q_\infty x^2 + \dots \right], \quad (11)$$

and the incompressibility,

$$K(x) = (1 + 3x) \left[K_\infty + (9K_\infty + Q_\infty)x + 6Q_\infty x^2 + \dots \right]. \quad (12)$$

Fig. 4 displays the binding energy Eq. (10), pressure Eq. (11) and incompressibility Eq. (12) as function of the density ρ going from 0 to 0.2 fm^{-3} , for typical values for the quantities : $E_\infty = -16 \text{ MeV}$, $K_\infty = 240 \text{ MeV}$ and $Q_\infty = 350 \text{ MeV}$. The different curves correspond to various approximations in the density expansion of the binding energy Eq. (10). For instance, the solid line in the binding energy E/A corresponds to the 0-th order in the density expansion Eq. (10) where only the quantity E_∞ has been included, all other quantities being set to zero. The dotted-line (E+K) takes into account the quantities E_∞ and K_∞ , and the dashed line (E+K+Q) includes the quantities E_∞ , K_∞ and Q_∞ . Similar approximations have been performed in the case of the pressure Eq. (11) and incompressibility Eq. (12). A good convergence is found when successively including in the expressions for the binding energy, the pressure and the incompressibility the quantities E_∞ , K_∞ and Q_∞ . These quantities describe the density dependence of the equation of state and are given in table II for a set of models considered in this work.

It is clear from Table II that while the quantities E_∞ and K_∞ are not varying by more than 20%, the values

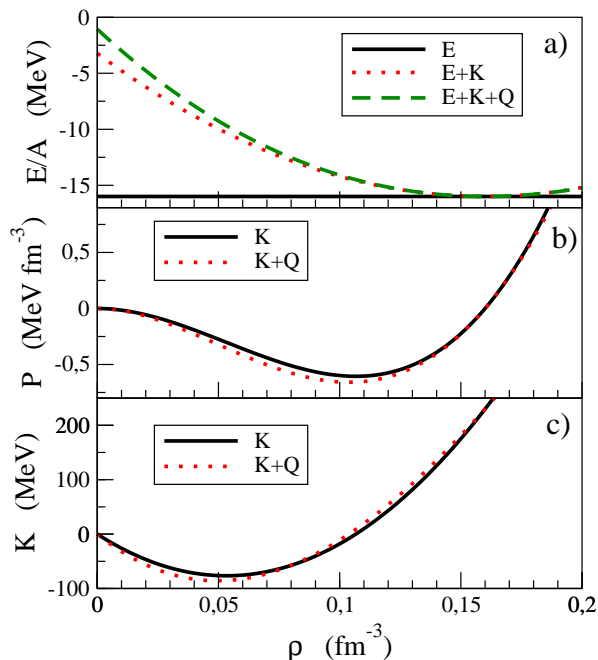


FIG. 4. (color online) a) Binding energy E/A in MeV, b) pressure in MeV fm^{-3} and c) incompressibility K in MeV, as a function of the density for various truncation in the expansion Eq. (10). See text for more details.

	ρ_0	E_∞	K_∞	Q_∞
	fm^{-3}	MeV	MeV	MeV
SLy5	0.160	-15.98	230	-363
SkM*	0.160	-15.79	217	-386
Sk255	0.157	-16.35	255	-350
Sk272	0.155	-16.29	272	-306
D1S	0.163	-16.02	210	-596
NL3	0.148	-16.24	271	189
DDME2	0.152	-16.14	251	478
FSUGold	0.148	-16.30	229	-537

TABLE II. Parameters appearing in the density expansion of the binding energy E/A Eq. (10) for a set of models considered in this work: ρ_0 is the saturation density, E_∞ the binding energy, K_∞ the incompressibility modulus, and Q_∞ the skewness parameter.

for the skewness parameter Q_∞ is almost unconstrained and can vary by more than 100% among the models. The uncertainty in the determination of the skewness parameter Q_∞ gives, in a quantitative way, the main lack of knowledge in the density dependence of the equation of state. The uncertainty on Q_∞ also impacts the density dependence of the pressure and more, interestingly here, of the incompressibility.

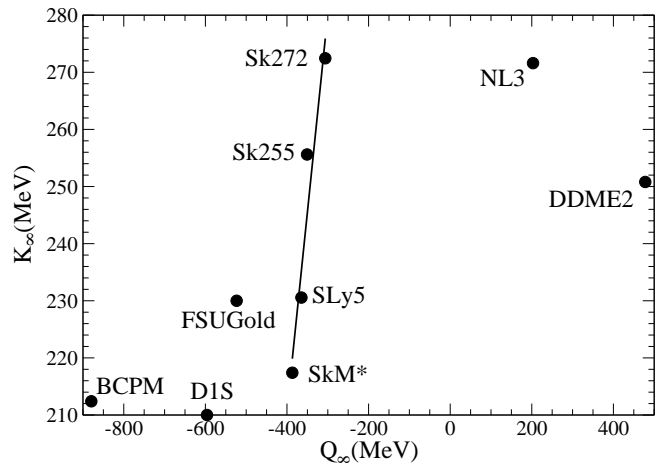


FIG. 5. K_∞ versus Q_∞ for several models. The solid line corresponds to the fit on the Skyrme EDFs values.

B. Stability of K_c

Let us now provide an explanation for the stability of K_c observed in Table II. From Eq. (12), and assuming the validity of a density expansion from ρ_0 to ρ_c , we obtain

$$K_c \simeq (1 + 3x_c) [(1 + 9x_c)K_\infty + (1 + 6x_c)x_c Q_\infty], \quad (13)$$

with $x_c = (\rho_c - \rho_0)/(3\rho_0)$.

In the case of Skyrme interaction, there is a good correlation among the quantities K_∞ and Q_∞ , as shown in Fig. 5. The parameters K_∞ and Q_∞ are mostly determined by the same term, the term t_3 in ρ^α , in the case of Skyrme interaction [10]. Due to their similar density dependence (in ρ^α), the Skyrme EDFs exhibit indeed a linear correlation among these two quantities whereas the picture is blurred when considering at the same time Skyrme and relativistic EDFs. The linear correlation among the Skyrme EDFs can be described by,

$$K_\infty = a + bQ_\infty, \quad (14)$$

with $a = 338 \pm 9$ MeV and $b = 0.29 \pm 0.03$. Injecting (14) in Eq. (13), one gets

$$K_c \simeq (1 + 3x_c) [(1 + 9x_c)a + f(x_c)Q_\infty], \quad (15)$$

with $f(x) = (6x^2 + (9b + 1)x + b)$. An EDF-almost-independent value of K_c is therefore obtained for $f(x)=0$ since Q_∞ is the only EDF-dependent quantity in Eq. (15): the solution of $f(x)=0$ shall therefore provide the crossing point observed on Fig. 1. The function $f(x)$ has only one zero for positive densities, given by $x_c = -0.095 \pm 0.002$, which corresponds to $\rho = (0.714 \pm 0.005)\rho_0 = \rho_c$.

In the Skyrme case there is therefore a density, ρ_c , for which the incompressibility modulus $K(\rho_c)$ is independent from the quantities K_∞ and Q_∞ defined in Eq. (10),

and is

$$K_c \equiv K(\rho_c) = (1 + 3x_c)(1 + 9x_c)a = \frac{\rho_c}{\rho_0}(3\frac{\rho_c}{\rho_0} - 2)a. \quad (16)$$

Taking the value for a given by the linear correlation, one finds $K_c = 34 \pm 4$ MeV, confirming the value of the crossing point shown in Table I and on Fig. 1 for the Skyrme EDFs. This approach confirms in a both quantitative and qualitative way the existence of a crossing point, especially in the case of the Skyrme EDF. In the case of the other EDFs, it is rather a crossing area that is obtained (Fig. 1), due to their various density dependence, as discussed above.

C. Relation between K_∞ and M_c

Fig. 6 displays the (M_c, K_∞) correlation for four Skyrme EDFs. Adding to this correlation graph EDFs with other density dependences, such as the relativistic one, drastically blurs this correlation. This shall originates from the large uncertainty on the value of the skewness parameter Q_∞ among the EDFs discussed in the previous section (Table II). Using Eqs. (7), (8) and (12), the quantity M_c can be expressed as,

$$M_c \simeq 3K_c + (1 + 3x_c)^2 [9K_\infty + (1 + 12x_c)Q_\infty]. \quad (17)$$

The correlation between M_c and K_∞ depends on the density dependence of the binding energy reflected in the skewness parameter Q_∞ , which can vary to a large extent, see Table II. More precisely, from Eq. (17), one can deduce the value of the quantity K_∞ as,

$$K_\infty = \frac{1}{9} \frac{M_c - 3K_c}{(1 + 3x_c)^2} - \frac{1 + 12x_c}{9} Q_\infty, \quad (18)$$

where the second term of the r.h.s shows the theoretical error on K_∞ induced by the uncertainty on Q_∞ , the unconstrained density dependence of the EoS. K_c and x_c are fixed by the existence of a crossing point, and M_c is extracted from the correlation analysis based on the experimental E_{GMR} . It is therefore clear that the uncertainty on K_∞ is related to the lack of knowledge on the density dependence of the equation of state, represented in the present analysis by the skewness parameter Q_∞ . Taking a typical uncertainty for Q_∞ of ± 400 MeV (Table II), Eq. (18) provides a variation on K_∞ about ± 40 MeV, compatible with the present uncertainty on K_∞ .

In conclusion, the relation Eq. (18) clearly shows that the uncertainty on the incompressibility modulus K_∞ is mainly related to that on the quantities Q_∞ . The reduction of the error bar on K_∞ is therefore mostly related to a better knowledge of the skewness parameter Q_∞ , for which new experimental constraints shall be found. On the contrary the density dependence around the crossing point M_c can be more directly constrained from E_{GMR} , as it will be showed below.

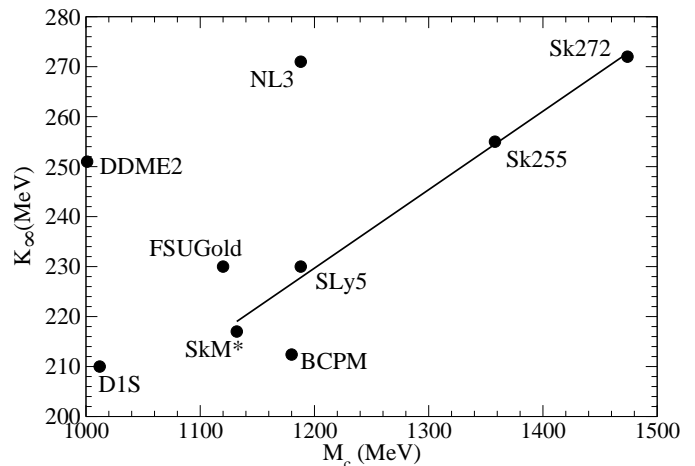


FIG. 6. K_∞ as a function of M_c for various Skyrme, Gogny and relativistic functionals

IV. A SIMPLE EXPRESSION RELATING E_{GMR} AND M_c

To provide a complementary view to microscopic approaches [1–10], it may be useful to derive an analytic relationship between the GMR centroid in nuclei and the quantity M_c , in order to enlighten and confirm the results obtained with a fully microscopic approach, see Sec. II and Ref. [10]. In this section we aim to derive an analytical relationship between the centroid of the GMR and the relevant quantity of the EoS, M_c Eq. (7).

The energy centroid of the GMR is used to define the incompressibility in nuclei K_A [1]:

$$E_{\text{GMR}} = \sqrt{\frac{\hbar^2 K_A}{m \langle r^2 \rangle}}. \quad (19)$$

In order to derive an analytical relationship, $\langle r^2 \rangle$ can be approximated by $3R^2/5$ [32] where $R \simeq 1.2A^{1/3}$ is the nuclear radius, yielding:

$$E_{\text{GMR}} \simeq \frac{\hbar}{R} \sqrt{\frac{5K_A}{3m}} \quad (20)$$

We shall derive an analytic relation between K_A and M_c using the LDA, in order to check, in a complementary way to microscopic approaches, the role of M_c in determining the centroid of the GMR.

The following step consists in dividing K_A into a nuclear and a Coulomb contributions, as

$$K_A = K_{\text{Nucl}} + K_{\text{Coul}} \cdot Z^2 A^{-4/3} \quad (21)$$

where, in the liquid drop approach, K_{Nucl} is defined as

$$K_{\text{Nucl}} = K_\infty + K_{\text{surf}} A^{-1/3} + K_\tau \left(\frac{N - Z}{A} \right)^2,$$

as in the Bethe Weissäcker formula for the binding energy [1]. The accuracy of this approach can be enhanced with the inclusion of higher order terms [33]. The quantities K_∞ , K_{surf} and K_τ are however poorly constrained by the relative small data [1, 34]. We prefer instead to extract K_{Nucl} from the LDA which has the advantage that i) it was proven to be a good approximation of the microscopic calculation [12], and ii) the consistency between the value obtained for K_A and the Skyrme functional is guaranteed.

A. The local density approximation (LDA)

The nuclear contribution K_{Nucl} is related to the density dependence of the incompressibility $K(\rho)$ as [12],

$$K_{\text{Nucl}} = \frac{\rho_0^2}{A} \int d^3r \frac{K(\rho(r))}{\rho(r)} \quad (22)$$

Eq. (22) allows to perform the LDA by considering the density profile of nuclei, $\rho_A(r)$, in Eq. (8), where $\rho = \rho_A(r)$. The LDA give accurate estimation of K_{Nucl} [12]. It should be noted that in Eq. (22), the value of $K(\rho)$ at saturation density (i.e. K_∞) doesn't have any specific impact on the K_A value and therefore nor on the prediction of E_{GMR} . Further, due to the ex-

istence of the crossing area $(\rho_c, K_c) \simeq (0.1 \text{ fm}^{-3}, 40 \text{ MeV})$, which takes into account both the Skyrme EDFs crossing (Table I) and the relativistic one (Fig 1), $K(\rho)$ can be approximated to the first order around the crossing point by:

$$K(\rho) = \frac{M_c \rho}{3\rho_c} - \frac{M_c}{3} + K_c \quad (23)$$

where M_c is related to the first derivative of the incompressibility, Eq. (7).

This first order approximation is relevant as observed on the (E_{GMR}, M_c) correlation of Figs. 2 and 3. Of course taking the density dependence of the incompressibility as its first derivative around the crossing point remains an approximation, which explains the non exactly linear (E_{GMR}, M_c) correlation on Fig. 2 considering Skyrme and relativistic EDFs. But still, the correlation among the EDF families (Skyrme, Relativistic) are ordered.

The integral in Eq. (22) is taken between $\rho_0/2$ and ρ_0 , which is adapted to the linear regime around ρ_c and corresponds to the typical dispersion of the density values around the mean density in nuclei [10]. Injecting expression (23) in (22) and assuming a Fermi shape of the nuclear density, with diffusivity $a \simeq 0.5 \text{ fm}$ [32], yield the analytical relation between the centroid of the GMR and M_c , using Eq. (20) and (21):

$$E_{\text{GMR}} = \frac{\hbar}{R} \left\{ \frac{20\pi}{3mA} \int_{\rho_0/2}^{\rho_0} \left[a \ln \left(\frac{\rho_0}{\rho} - 1 \right) + R \right]^2 \left(\frac{M_c \rho}{3\rho_c} - \frac{M_c}{3} + K_c \right) \frac{a}{1 - \rho/\rho_0} \frac{\rho_0^2}{\rho^2} d\rho + \frac{5K_{\text{Coul}}}{3m} Z^2 A^{-4/3} \right\}^{1/2} \quad (24)$$

The integral in Eq. (24) denotes the nuclear contribution whereas the second part comes from the Coulomb effects. The Coulomb contribution is evaluated using $K_{\text{Coul}} = -5.2 \text{ MeV}$ [1, 35]. This value is obtained from the liquid drop expansion of the incompressibility and applied to several Skyrme interactions [35]. It should be noted that the Fermi shape is a good approximation of the density and we have checked that the diffusivity of the density obtained from microscopic Hartree-Fock calculations (0.47 fm) is very close to 0.5 fm. The use of the Fermi density is legitimized by the aim of tracing the analytical impact of the quantity M_c on the GMR centroid. Equation (24) also underlines the important role of the quantity M_c on the GMR centroid. On the contrary, the incompressibility at saturation density K_∞ doesn't play any specific role in Eq. (24). It is therefore rather the quantity M_c which is the relevant quantity to be constrained by the GMR measurements.

B. Results and comparison with the microscopic method

The stability of the results obtained with Eq. (24) has been studied with respect to the diffusivity value a , the LDA prescription (Eq. (22)), the crossing point (ρ_c, K_c) values and the integration range. A sound stability is obtained against these quantities: the predicted GMR centroid doesn't change by more than 10 % by making all these variations in relevant physical ranges.

We first study the behavior of the nuclear contribution ($K_{\text{Coul}} = 0$ in Eq. (24)). Fig. 7 displays the correlation between the centroid of the GMR and the M_c value using Eq. (24), for nuclei with $A=208$ and $A=120$. A good qualitative agreement is obtained with the fully microscopic results (see Fig. 2 and 3) in view of the approximations performed to derive Eq. (24). The A -dependence is also well described. These results confirm the validity of the present approach, and emphasize M_c as a relevant EoS quantity to be constrained by the GMR measurements. It also qualitatively agrees with the microscopic results.

In order to perform a more quantitative study, the

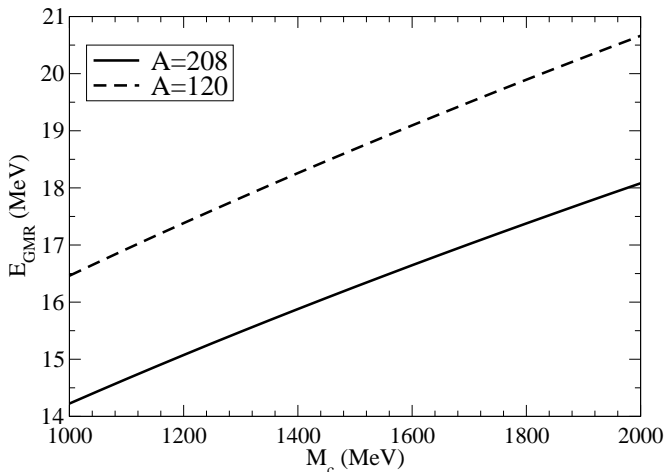


FIG. 7. Centroid of the GMR in $A=208$ (solid line) and $A=120$ (dashed line) nuclei calculated with the local density approximation for the nuclear incompressibility and using its first derivative at the crossing point (Eq. (24) without the Coulomb term).

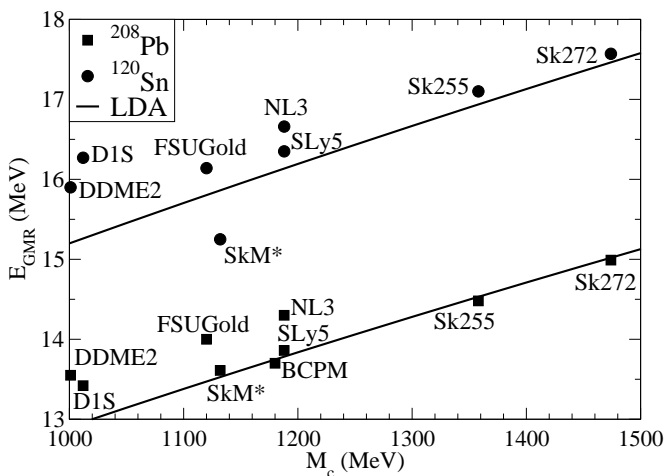


FIG. 8. Centroid of the GMR in ^{208}Pb and ^{120}Sn calculated with the LDA and including the Coulomb effects (solid lines, see text) as a function of M_c . The values for various EDFs obtained microscopically (squares and dots) are also displayed for comparison.

curves on Fig. 8 displays the centroid of the GMR in ^{208}Pb and ^{120}Sn nuclei predicted using the full Eq. (24) with both the nuclear and the Coulomb contributions. The comparison with the microscopic results using various EDFs is also shown. A good agreement is obtained in both cases, strengthening again the present analytical LDA approach, and emphasising the role of M_c . Comparing Figs. 7 and 8, the Coulomb effect on the GMR centroid can be evaluated to be about 1 MeV in heavy nuclei.

The almost linear correlation between E_{GMR} and M_c

observed on Fig. 8 can be further investigated. Eq. (24) can be rewritten as:

$$E_{\text{GMR}} = (\alpha(A, \rho_0)M_c + \beta(A, Z, \rho_0))^{1/2} \quad (25)$$

with

$$\alpha(A, \rho_0) \equiv \frac{20\pi\hbar^2}{9mAR^2} \int_{\rho_{\min}}^{\rho_0} \left[a \ln \left(\frac{\rho_0}{\rho} - 1 \right) + R \right]^2 \times \left(\frac{\rho}{\rho_c} - 1 \right) \frac{a}{1 - \rho/\rho_0} \frac{\rho_0^2}{\rho^2} d\rho \quad (26)$$

$$\beta(A, Z, \rho_0) \equiv \frac{5\hbar^2 K_{\text{Coul}}}{3mR^2} Z^2 A^{-4/3} + \frac{20\pi\hbar^2}{3mAR^2} \int_{\rho_{\min}}^{\rho_0} \left[a \ln \left(\frac{\rho_0}{\rho} - 1 \right) + R \right]^2 \frac{aK_c}{1 - \rho/\rho_0} \frac{\rho_0^2}{\rho^2} d\rho \quad (27)$$

Fixing ρ_c and K_c , the coefficients α and β only depend on the nucleus' mass and charge (A, Z), and on the saturation density ρ_0 , which is constrained by the charge radii. Typical values are $\alpha=0.12$ MeV and $\beta=42$ MeV² in the case of ^{208}Pb and $\alpha=0.16$ MeV and $\beta=75$ MeV² in the case of ^{120}Sn .

It should be noted that the LDA approximation (25) of E_{GMR} can be obtained because of the existence of the crossing point. In Eq. (25), the energy of the GMR depends on the functional mostly through the parameter M_c . In conclusion, the LDA allows to obtain expression (25) relating E_{GMR} with M_c in a simple and accurate form.

Introducing (M_0, E_0) as the reference point, where $M_0 \equiv 1200$ MeV and E_0 is the corresponding GMR energy, one can go one step further and linearise Eq. (25) with respect to $M_c - M_0$, as

$$E_{\text{GMR}} \simeq \frac{\alpha}{2E_0} M_c + \left(E_0 - \frac{\alpha M_0}{2E_0} \right) \quad (28)$$

This is justified for the typical values of M_c , ranging between 1000 MeV and 1500 MeV as shown on Fig. 8. The almost linear correlation between E_{GMR} and M_c observed on Fig. 8 is therefore understood by the present approach (Eq. (28)). It clearly shows that the measurement of the GMR position constrains M_c , which is a first information on the density dependence of the incompressibility. It should be recalled that such a quantitative description is not possible with K_∞ because there is no crossing point of the incompressibility at saturation density: Eq. (24) is not applicable in that case.

V. CONCLUSIONS

The relationship between the isoscalar GMR and the equation of state raises the question of which EoS quantity is constrained by GMR centroid measurements. The

incompressibility modulus K_∞ alone may not be the relevant one nor the most direct because the more general density dependence of the incompressibility should be considered. A crossing area is observed on $K(\rho)$ at $\rho_c \simeq 0.1 \text{ fm}^{-3}$ among various functionals. Using a microscopic approach, such as constrained-HFB, the slope M_c of $K(\rho)$ at the crossing density can be directly constrained by GMR measurements. This shall assess the change of the method in extracting EoS quantities from GMR: M_c is first constrained, and an approximate value of K_∞ can be deduced in a second step [10].

The stability of K_c has been demonstrated in the case of Skyrme EDFs. A general relationship between M_c and K_∞ is obtained, showing the contribution of the uncertainty in the density dependence of the EoS which has been casted into the quantities Q_∞ . The K_∞ value can be determined in a second step from the knowledge of the M_c value, requiring a better constraint on the skewness parameter Q_∞ , being the main uncertainty for the density dependence of the incompressibility between the crossing density and the saturation density. One should recall that the K_∞ value remains $230 \pm 40 \text{ MeV}$ (17% uncertainty), whereas the quantity M_c is better constrained

to be $M_c = 1100 \pm 70 \text{ MeV}$ (6% uncertainty) [10]. A better knowledge of higher order density dependent terms of $E/A(\rho)$, e.g. the skewness parameter Q_∞ , shall help to more accurately relate the parameter M_c to the incompressibility modulus K_∞ .

Using the LDA approach and an analytical approximation of the density, the microscopic results have been confirmed: the measurement of the centroid of the isoscalar giant monopole resonance constrains the first derivative M_c of the incompressibility around the crossing point $\rho_c \simeq 0.1 \text{ fm}^{-3}$. A analytical relation between the centroid of the GMR and the quantity M_c is derived and the predicted GMR centroid are found in good agreement with the microscopic method.

ACKNOWLEDGEMENT

The authors thank I. Vidaña for fruitful discussions. This work has been partly supported by the ANR SN2NS contract, the Institut Universitaire de France, and by CompStar, a Research Networking Programme of the European Science Foundation.

-
- [1] J.-P. Blaizot, Phys. Rep. 64, 171 (1980).
 [2] D. Vretenar, T. Niksic and P. Ring, Phys. Rev. C68, 024310 (2003).
 [3] B.K. Agrawal, S. Shlomo and V. Kim Au, Phys. Rev. C68, 031304(R) (2003).
 [4] G. Colò, N. Van Giai, J. Meyer, K. Bennaceur, P. Bonche, Phys. Rev. C70, 024307 (2005).
 [5] J. Piekarewicz, Phys. Rev. C76, 031301(R) (2007).
 [6] T. Li, U. Garg, Y. Liu, R. Marks, B.K. Nayak, P.V. Madhusudhana Rao, M. Fujiwara, H. Hashimoto, K. Kawase, K. Nakanishi, S. Okumura, M. Yosoi, M. Itoh, M. Ichikawa, R. Matsuo, T. Terazono, M. Uchida, T. Kawabata, H. Akimune, Y. Iwao, T. Murakami, H. Sakaguchi, S. Terashima, Y. Yasuda, J. Zenihiro, and M. N. Harakeh, Phys. Rev. Lett. 99, 162503 (2007).
 [7] J. Li, G. Colò and J. Meng, Phys. Rev. C78, 064304 (2008).
 [8] E. Khan, Phys. Rev. C80, 011307(R) (2009).
 [9] P. Veselý, J. Toivanen, B.G. Carlsson, J. Dobaczewski, N. Michel, and A. Pastore, Phys. Rev. C86, 024303 (2012).
 [10] E. Khan, J. Margueron and I. Vidaña, Phys. Rev. Lett. 109, 092501 (2012).
 [11] O. Civitarese, A.G. Dumrauf, M. Reboiro, P. Ring, M.M. Sharma, Phys. Rev. C43, 2622 (1991).
 [12] E. Khan, J. Margueron, G. Colò, K. Hagino and H. Sagawa, Phys. Rev. C82, 024322 (2010).
 [13] Li-Gang Cao, H. Sagawa, G. Colò, Phys. Rev. C86, 054313 (2012).
 [14] N. Paar, D. Vretenar, E. Khan, G. Colò, Rep. Prog. Phys. 70, (2007) 691.
 [15] D.J. Thouless, Nucl. Phys. 22, 78 (1961).
 [16] O. Bohigas, A.M. Lane and J. Martorell, Phys. Rep. 51, 267 (1979).
 [17] L. Capelli, G. Colò and J. Li, Phys. Rev. C79, 054329 (2009).
 [18] A.L. Fetter and J.D. Walecka, Quantum Theory of Many-Particle Systems, McGraw-Hill, New York, 1971.
 [19] J. Piekarewicz, Phys. Rev. C83, 034319 (2011).
 [20] B.A. Brown, Phys. Rev. Lett. 85, 5296 (2000).
 [21] S. Typel and B.A. Brown, Phys. Rev. C64, 027302 (2001).
 [22] E. Khan, M. Grasso and J. Margueron, Phys. Rev. C80, 044328 (2009).
 [23] C. Horowitz, Z. Ahmed, C.-M. Jen, et al., Phys. Rev. C85, 032501 (2012).
 [24] G.A. Lalazissis, J. Konig and P. Ring, Phys. Rev. C 55, 540 (1997).
 [25] G.A. Lalazissis, T. Niksic, D. Vretenar, P. Ring, Phys. Rev. C 71, 024312 (2005).
 [26] J. Bartel, P. Quentin, M. Brack, C. Guet, H.-B. Hakansson, Nucl. Phys. A386, 79 (1982).
 [27] J.F. Berger, M. Girod and D. Gogny, Comp. Phys. Comm. 63, 365 (1991).
 [28] E. Chabanat, P. Bonche, P. Haensel, J. Meyer, R. Schaeffer, Nucl. Phys. A635, 231 (1998).
 [29] M. Baldo, L.M. Robledo, P. Schuck, X. Viñas, arXiv:1210.1321.
 [30] C. Ducoin, J. Margueron, & C. Providência, Europhys. Lett. 9, 32001 (2010).
 [31] C. Ducoin, J. Margueron, C. Providência, & I. Vidaña, Phys. Rev. C 83, 045810 (2011).
 [32] P. Ring, P. Schuck, The Nuclear Many-Body Problem, Springer-Verlag, Heidelberg, (1980).
 [33] S.K. Patra, M. Centelles, X. Viñas and M. Del Estal, Phys. Rev. C65 (2002) 044304.
 [34] J. M. Pearson, N. Chamel, S. Goriely, Phys. Rev. C82, 037301 (2010).

- [35] H. Sagawa, S. Yoshida, Guo-Mo Zeng, Jian-Zhong Gu, and Xi-Zhen Zhang, *Phys. Rev. C* **76**, 034327 (2007).